Effect of Irradiation Sources and Oxygen Concentration on the Photocatalytic Oxidation of 2-Propanol and Acetone Studied by In Situ FTIR

ARTICLE *in* THE JOURNAL OF PHYSICAL CHEMISTRY B · MAY 2003

Impact Factor: 3.3 · DOI: 10.1021/jp025995h

3 AUTHORS, INCLUDING:

Daniel Raftery
University of Washington Seattle
181 PUBLICATIONS **4,888** CITATIONS

SEE PROFILE

Effect of Irradiation Sources and Oxygen Concentration on the Photocatalytic Oxidation of 2-Propanol and Acetone Studied by in Situ FTIR

Weizong Xu,† Daniel Raftery,* and Joseph S. Francisco*

H. C. Brown Laboratory, Department of Chemistry, Purdue University, West Lafayette, Indiana 47907-1393

Received: April 23, 2002; In Final Form: February 28, 2003

The photocatalytic oxidation (PCO) of 2-propanol and acetone was studied on TiO_2 powder at high coverage (>2 monolayers) at various oxygen concentrations using in situ FTIR. Two UV irradiation sources, either a continuous-wave UV lamp or an excimer laser, were applied to investigate the effect of the UV source on the PCO. It was found that higher oxygen concentrations increased the PCO rate of 2-propanol and acetone. The excimer laser source accelerated the PCO rate of 2-propanol while decelerating that of acetone as compared to the continuous-wave source. This effect was found to be larger at higher oxygen concentrations. Factors such as multiphoton adsorption or a pulsed irradiation were excluded as possible explanations for the irradiation source effect. More likely, the laser source changes the reaction mechanism by introducing an abrupt temperature increase, and hence the thermal decomposition, that is, dehydration of 2-propanol to propene, is effectively initiated on the surface. The PCO of 2-propanol was found to proceed along two routes: one was through the chemisorbed species, 2-propoxide, to form CO_2 directly; the other was through conversion of H-bonded 2-propanol to acetone, followed by thermal fragmentation of mesityl oxide (aldol condensation product of acetone) to form formate species, and finally to CO_2. It was also found that the acetone decay rate during acetone PCO was much faster than that of acetone formed as an intermediate during 2-propanol PCO at the same oxygen concentration. This was likely due to the presence of other species competing for reaction sites on the catalyst surface.

1. Introduction

The widespread use of volatile organic compounds (VOCs) has caused a number of significant environmental problems that include photochemical smog and atmospheric ozone production. In recent decades, much attention has been focused on developing measures to convert these pollutants into nontoxic compounds. Among these detoxification measures, heterogeneous semiconductor photocatalytic oxidation (PCO) has been found to be an efficient way to transform many of these VOCs into nontoxic compounds, such as CO_2 and H_2O. Although PCO has been studied and applied for a few decades, a complete understanding of the complex reaction picture is still elusive. A number of researchers have reviewed the important features and summarized the research progress regarding PCO at both liquid−solid and gas−solid interfaces.[1−3] Many factors affect and complicate the PCO process and currently limit its more widespread use. These factors include the effect of chemical properties of VOCs on the catalytic efficiency, the bulk and surface characteristics of the semiconductor catalysts, the type and intensity of the light source, the presence of surface-adsorbed water, and the oxygen concentration, as well as others.

Ketones and alcohols have been regarded as the central classes of VOCs responsible for poor air quality because these compounds comprise the most widely used organic solvents.[4−7] In addition, acetone is a major intermediate during 2-propanol PCO, and therefore, understanding its PCO process is important. Falconer and co-workers[8] have conducted detailed studies on the kinetics of the 2-propanol PCO on TiO_2 powder by temperature-programmed desorption/temperature-programmed oxidiation and concluded that the PCO of 2-propanol proceeded through acetone as an intermediate, followed by the slow oxidation of acetone to final products, CO_2 and H_2O. Although they suggested the possible formation of surface intermediates during oxidation, no direct evidence was found. Grassian and co-workers[9] reported studies of acetone PCO as a function of acetone coverage, oxygen pressure, and water adsorption. They found that the formation of mesityl oxide, the product of acetone aldol condensation, was proportional to the acetone surface coverage. Furthermore, the water adsorption could greatly decrease the formation of mesityl oxide. The studies by Raupp and Junio[10] on acetone PCO showed that its oxidation rates strongly depended on UV intensity, and the measured quantum yields greater than one suggested that oxidation occurred through free radical chain reactions mediated by surface complexes. We have recently performed detailed PCO studies of 2-propanol[11] and acetone[12] on TiO_2 catalysts with different morphologies using solid-state NMR (SSNMR). We found that the chemisorbed species 2-propoxide is responsible for the fast PCO observed on TiO_2 powder, while 2-propoxide does not form on a TiO_2 monolayer catalyst anchored on porous Vycor glass (TiO_2/PVG). We also found that acetone PCO proceeded at a very slow rate through the formation of mesityl oxide on the dehydrated TiO_2 powder. Mesityl oxide then fragmented to form formic acid,[12] which subsequently reacted with a surface OH group to form titanium formate and was further oxidized to the final product CO_2.

In this paper, we report a kinetic study of 2-propanol and acetone PCO on dehydrated TiO_2 powder using two UV light sources, a continuous-wave UV lamp and a UV laser source.

* To whom correspondence should be addressed. E-mail addresses: raftery@purdue.edu; jfrancis@purdue.edu.

† Present address: Alcoa Technical Center, Pittsburgh, PA 15069.

10.1021/jp025995h CCC: $25.00
Published on Web 04/17/2003

In a previous study, we noted that the use of pulsed laser irradiation could profoundly change the product distribution and kinetics of PCO.[13] It is well-known since the 1960s that pulsed or flashed illumination can produce rapid acetone decomposition during its photolysis through radical intermediates.[14,15] By utilizing these intense light sources, such as a flash lamp, a spark, an exploding wire, or even a laser source, the reaction can be simplified by second-order radical reactions due to the high density of free radicals produced ($^{\bullet}CH_3CO$ and $^{\bullet}CH_3$). In this study, a continuous UV lamp and a pulsed UV laser source are applied to observe their effect on the PCO of 2-propanol and acetone. In addition, the effect of oxygen concentration on PCO of 2-propanol and acetone at high coverage, greater than 2 monolayers (ML), was also investigated. The results observed point to the participation of a thermal reaction pathway in the pulsed experiments.

2. Experiment

2.1. FTIR Cell. An FTIR reaction cell was constructed to allow the simultaneous irradiation of the TiO_2 catalyst by UV source and in situ IR detection of reaction and was based on a design originally developed by Yates and co-workers.[16−18] Briefly, the glass cell consisted of two quartz windows, two ZnS windows, and a sample holder. The pair of quartz windows was used for the effective UV irradiation, while the pair of ZnS windows was used for IR detection. These two pairs of windows were arranged for crossed beam irradiation. The front quartz window was set at Brewster's angle to allow the maximum UV light transmission into the cell. A connection to the cell allowed evacuation and loading of gaseous reactants. A tungsten mesh was used to support the catalyst and was connected to a ceramic sample holder so that the sample could be heated electrically. A thermocouple was attached to the mesh so that the temperature over the catalyst could be monitored while heating occurred. The reaction cell had a volume of approximately 100 cm^3.

2.2. Catalyst Preparation. The catalyst samples were made by spraying a slurry of TiO_2 powder (Degussa P25, approximately 70% anatase and 30% rutile, BET surface area 55 $m^2\ g^{-1}$) onto a tungsten mesh. The TiO_2 slurry was prepared by sonically dispersing 1 g of TiO_2 powder into a mixture of 10 mL of deionized water and 90 mL of acetone. The TiO_2-coated mesh was then calcined in the presence of O_2 at 500 °C for 8 h to provide a clean and dry catalytic surface. Approximately 25 mg of TiO_2 powder was evenly coated onto the 2 cm × 2 cm grid.

2.3. In Situ FTIR Method. Once the catalyst was calcined, the tungsten mesh, along with the supported catalyst, was mounted onto the sample holder within the reaction cell at a 45° angle with respect to both the UV and IR beams. The IR cell was then evacuated to approximately 10^{-3} Torr. The catalyst was heated electrically to 370−410 K for a few hours to remove any remaining contaminants on the catalyst surface due to its brief exposure to air. The cell was then allowed to cool to room temperature under a vacuum at 10^{-5} Torr for a few hours before the introduction of any gas compounds. A background FTIR spectrum was obtained at this point, after which the gas sample was introduced into the cell, and the pressure of acetone, 2-propanol, or oxygen could be monitored by a Varian millitorr thermocouple vacuum gauge (10^{-2} to 100 Torr). The reagent amount was then calculated according to the calibrated volume of the cell. Changes in the spectra during the surface adsorption of acetone or 2-propanol and their PCOs were then observed by in situ FTIR as a function of time. Typically, the FTIR spectra were obtained every 15 min during irradiation. Each spectrum consisted of an average of 16 scans and had a resolution of 1 cm^{-1}.

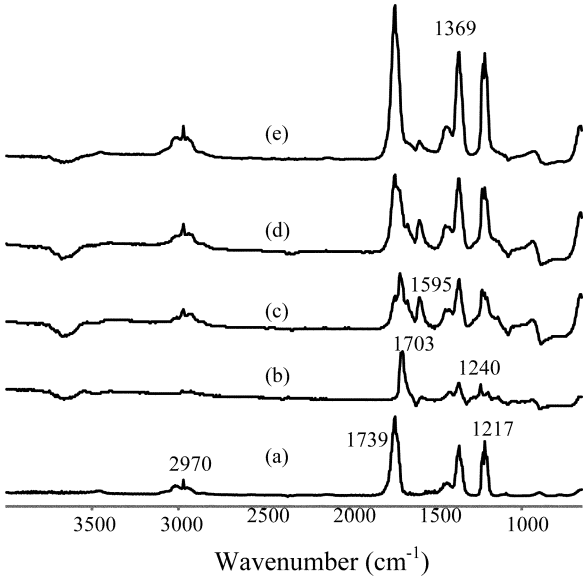

Figure 1. FTIR spectra of (a) gas-phase acetone and of acetone adsorbed on the TiO_2 surface at different surface coverages: (b) 0.15 ML; (c) 0.72 ML; (d) 1.14 ML; (e) 2.37 ML. Spectra were acquired approximately 30 min after acetone was adsorbed.

2.4. UV Sources. Two types of UV sources were utilized in these studies, either a broadband high-pressure 500 W Xe arc lamp (Oriel Corp.) or a Lambda Physik Compex 351 nm XeF excimer laser. The high-pressure Xe arc lamp was operated at 350 W output. A water cell and a heat-absorbing filter (KG1 Schott type, Melles Griot) were placed in front of the lamp to absorb near-IR light and reduce sample heating. To avoid direct photolysis of the target compounds at short UV wavelengths, a UV filter was also placed in front of the reaction cell. For 2-propanol, which strongly absorbed photons at wavelengths below 250 nm, a UV filter with a cutoff wavelength of approximately 300 nm (WG295 Schott type) was selected. The power entering the reaction cell using this setup was measured to be approximately 2 W (Scientech power meter). Because the band gap of TiO_2 is 3.2 eV, the photons at wavelengths below approximately 385 nm would effectively initiate the PCO process. According to the emission spectrum of the Xe arc lamp,[19] approximately 10% of photons occur in the range of 320−385 nm, and therefore, the total power of photons effective for PCO is about 0.20 W. To compare the lamp's photon flux with that of the laser source, we assume that the latter's power is all at 351 nm, such that approximately 3.5×10^{17} photons/s irradiated the catalyst surface. The 351 XeF excimer laser (Lamda Physik Complex) was operated at a repetition rate of 15 Hz, a pulse width of 10 ns, and pulse energies between 5 and 80 mJ/pulse. The power entering the reaction cell at 60 mJ/pulse and 15 Hz was measured to be 0.25 W, which provided an average photon flux of 4.3×10^{17} photons/s.

3. Results and Discussion

3.1. Adsorption on TiO_2 Powder. *3.1.1. Acetone Adsorption.* Spectra of different acetone surface coverages (0.15, 0.72, 1.14, and 2.37 ML) adsorbed on TiO_2 are shown in Figure 1 after the adsorption process approached equilibrium (∼30 min). A calculation of the surface coverage based on BET analysis[12] indicated that the saturation coverage of acetone on TiO_2 powder is 5.0 molecules/nm^2. To compare the spectral features before and after the adsorption of acetone, the spectrum of pure gas-

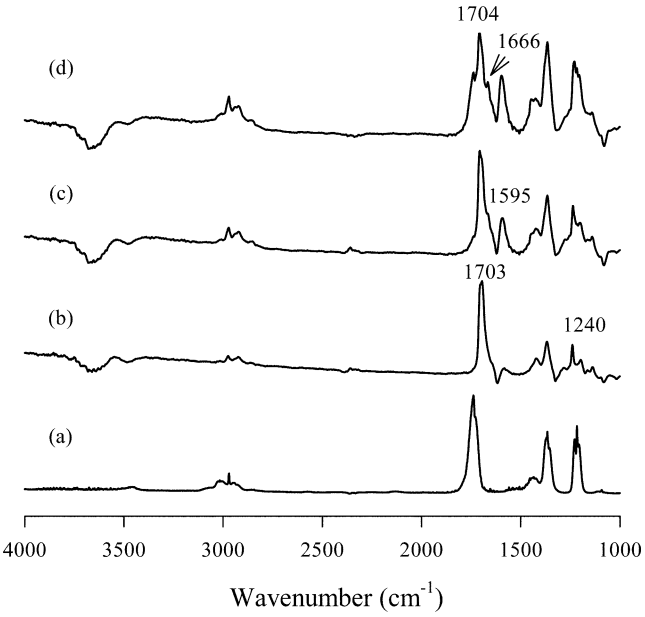

Figure 2. FTIR spectra of (a) gas-phase acetone and acetone (0.72 ML) adsorbed on the TiO_2 surface at different times after the introduction of acetone: (b) immediately; (c) 15 min; (d) 30 min.

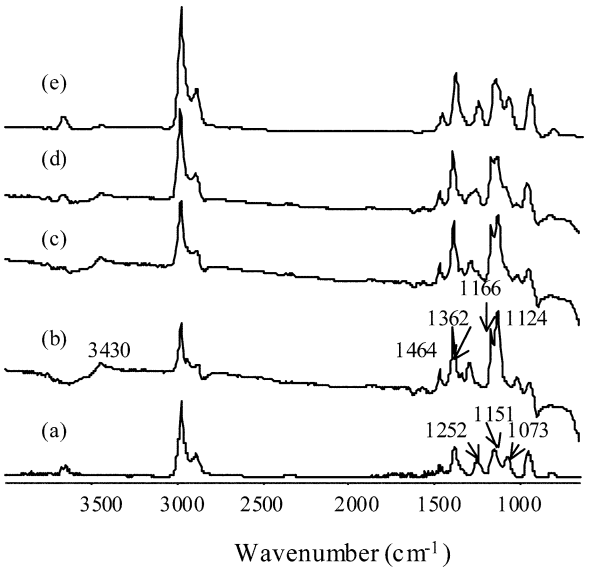

Figure 3. FTIR spectra of (a) gas-phase 2-propanol and 2-propanol adsorbed on TiO_2 surface at different surface coverages: (b) 0.9 ML; (c) 1.8 ML; (d) 3.0 ML; (e) 7.4 ML.

phase acetone (Figure 1a) is shown as well. At low surface coverage (0.15 ML), characteristic peaks at 1703 and 1240 cm^{-1} were the most prominent features in the spectrum (Figure 1b). Grassian assigned these peaks to adsorbed acetone on the TiO_2 surface.[9] The peak shift of the carbonyl stretch mode from 1739 cm^{-1} for gas-phase acetone to 1703 cm^{-1} indicated a relatively strong interaction between adsorbed acetone and surface OH groups. This was also suggested by the negative peaks in the range of 1500−1700 and 3500−3800 cm^{-1}, which indicated the reduction of isolated surface OH groups and their incorporation into hydrogen bonds. As the surface coverage increased, peaks at 1666 and 1595 cm^{-1} appeared and the peak at 1370 cm^{-1} increased in intensity. Grassian[9] ascribed the peaks at 1666 and 1595 cm^{-1} to mesityl oxide, the aldol condensation product of acetone on the TiO_2 surface. The peak around 1370 has been attributed to mesityl oxide as well.[20] Although the characteristic peaks of mesityl oxide on the surface in our FTIR spectrum are not very distinct because of overlapping peaks from gas-phase acetone, our SSNMR studies[12] showed clearly that (1) the formation of mesityl oxide is proportional to the surface coverage of acetone and (2) a small amount of formate species, resulting from the degradation of mesityl oxide that is very strongly adsorbed on the surface is formed. As a result, the surface species consisted of three components at saturation coverage, that is, adsorbed acetone, mesityl oxide, and formate species. Formate, which has broad IR peaks of 1555 and 1370 cm^{-1} when adsorbed at the TiO_2 surface,[21] may be present in our spectra, but these peaks are very difficult to distinguish given formate's low surface concentration and the presence of other surface species with similar bands. When the surface coverage was more than 1 ML, acetone peaks at 1217, 1370, 1739, and 2970 cm^{-1} become apparent (Figure 1d,e). The increased acetone coverage consists of a purely physisorbed layer, and therefore, the spectrum (Figure 1e) is very similar to that of gas-phase spectra.

It was also found that the adsorption of acetone on TiO_2 powder was relatively slow and took at least 30 min to reach equilibrium. The adsorption progression for acetone (0.72 ML) on TiO_2 powder can be seen clearly in Figure 2. An increase in the intensity of characteristic peaks of mesityl oxide (1666, 1595, and 1370 cm^{-1}) and the negative peaks in the range of 3500−3700 cm^{-1}, indicating surface hydrogen bond consumption, are evident as well.

3.1.2. 2-Propanol Adsorption. The spectra of 2-propanol at four different surface coverages are shown in Figure 3 after it was adsorbed on the TiO_2 powder surface. A calculation of the surface coverage based on BET analysis[11] indicated that the saturation coverage of 2-propanol on TiO_2 powder is 2.0 molecules/nm^2. To compare the spectral features before and after adsorption, the spectrum of pure gas-phase 2-propanol (Figure 3a) is shown as well. At a coverage less than 1 ML (0.9 ML) (Figure 3b), the relatively intense peaks at 1362, 1166, and 1124 cm^{-1} on the surface are ascribed to ν(CO), $\nu_{as}(CH_3)$, and $\nu_s(CH_3)$ of the chemisorbed species 2-propoxide.[22−25] The negative peaks in the range of 1500−1700 and 3600−3800 cm^{-1} indicate the consumption of surface OH groups due to the formation of hydrogen bonds with physisorbed 2-propanol and the formation of 2-propoxide. The positive peak at ~3430 cm^{-1} indicates the formation of water as the reaction product of 2-propanol and surface OH groups. This is in agreement with our previous SSNMR studies,[11] which showed that the first monolayer saturation coverage consists of chemisorbed 2-propoxide and H-bonded 2-propanol with limited mobility. As the surface coverage was increased, the second adsorbed monolayer of 2-propanol consisted of physisorbed 2-propanol molecules, which demonstrated high mobility, exchangeability with the adsorbed species in the first monolayer, or both processes.[11] As a result, it is not surprising that the IR peaks of physisorbed 2-propanol species (Figure 3c−e), which are similar to those of the gas phase (1252, 1151, and 1073 cm^{-1}),[23] increased in their intensity as a function of surface coverage. For the sample with 7.4 ML (Figure 3e), most of surface species are physisorbed 2-propanol within the system, and therefore, the observed spectrum is much like the gas-phase spectrum of 2-propanol (Figure 3a). By collecting the spectra at different time intervals after the adsorption of 2-propanol, it was found that the adsorption equilibrium of 2-propanol is much faster than that of acetone. It takes approximately 1 min to reach the adsorption equilibrium, while acetone takes at least 30 min.

3.2. Photocatalysis on TiO_2 powder. *3.2.1. PCO Control Experiments.* The oxidation/decomposition mechanisms can be complicated by different experimental conditions, which include

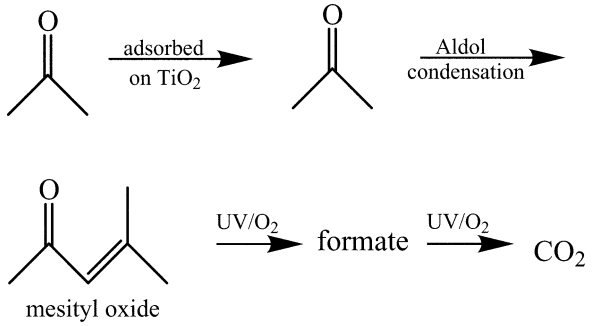

Figure 4. Illustration of the reaction mechanism for acetone photooxidation on TiO_2 powder.

oxygen concentration, light source type and intensity, temperature, catalyst morphology, and sample preparation. According to the UV absorption spectra (not shown), acetone absorbs at wavelengths below 350 nm while 2-propanol absorbs strongly at wavelengths below 250 nm. To avoid any direct photolysis of acetone/2-propanol, a filter with corresponding wavelength cutoff was placed in front of the FTIR cell. Without the TiO_2 catalyst, no oxidation of 2-propanol/acetone was observed under several hours of irradiation, even with O_2 present. Another control experiment was performed to observe whether lattice oxygen participates in the PCO of the target compound. The IR cell was pumped down to 10^{-5} Torr before introducing 2-propanol. The experiment was run without the addition of oxygen, and the Xe arc lamp was used as the UV source. We observed a slow conversion of 2-propanol to acetone. Previously, Larson et al. have observed PCO without added oxygen and attributed the reactivity to the participation of lattice oxygen.[8]

3.2.2. Oxygen Dependence. The PCO dependence of 2-propanol[8] and acetone[9] on O_2 concentration has been studied at low surface coverage (less than 1 ML). In the present study, we examined the oxygen dependence at relatively high surface coverages of 2-propanol and acetone to observe the behavior of physisorbed species during PCO. Approximately 20 μmol of 2-propanol (corresponding to 4.3 ML) or 28 μmol of acetone (corresponding to 2.4 ML) was introduced into the IR cell, and PCO reactions were followed using different oxygen concentrations.

3.2.2.1. PCO of Acetone. During the PCO of acetone under conditions of low O_2 concentration, no formation of CO_2 was observed. Similar findings were reported in our NMR experiments.[12] We have already shown that the PCO of acetone on dehydrated TiO_2 powder at low O_2 concentration occurred through mesityl oxide thermal fragmentation to formic acid, which forms titanium formate and a surface OH group and then the final product CO_2.[12] A reaction scheme is shown in Figure 4 that depicts the evolution of the acetone PCO. Formic acid with bands at 3185, 2945, 1728, and 1380 cm^{-1} [26] is difficult to observe in the presence of the other surface species using IR measurements, so we have not included it in the reaction scheme, although it is likely be present on the surface. The formation of mesityl oxide is proportional to the surface loading of acetone.[9,12] To observe the PCO of acetone at higher O_2 concentrations, we prepared a sample with an acetone surface coverage of approximately 2.4 ML. As we discussed above, there should be four species present after acetone is adsorbed on the TiO_2 surface: adsorbed acetone within the first saturation layer at 1703 cm^{-1}, mesityl oxide at 1666 and 1595 cm^{-1}, its fragmentation product formate species at 1555 and 1370 cm^{-1}, and physisorbed acetone at 1739 cm^{-1}. Changes in the peak widths observed during PCO, especially for the formate species, required the use of peak area measurements to monitor the changes in concentrations as a function of reaction time. The integration ranges chosen were 1620−1500 cm^{-1} for formate species and 2400−2225 cm^{-1} for CO_2. Because mesityl oxide (1595 cm^{-1}) and formate (1555 cm^{-1}) overlap somewhat, we were only able to monitor the appearance and disappearance of both species together. We know from our previous NMR studies that formate forms from mesityl oxide during PCO and is then slowly converted to CO_2.[12] In addition, the ν(C═O) peak due to adsorbed acetone overlaps the 1666 cm^{-1} peak of mesityl oxide, so we chose to integrate the two peaks together within the range of 1880−1620 cm^{-1}. A representative kinetic plot of the acetone PCO is shown in Figure 5 and shows the decay of acetone and mesityl oxide, formation of CO_2, and evolution of the formate species as an intermediate. Note that because of the difficulty of determining surface concentrations using IR intensities the integration areas for each of the peaks are normalized. The integration area of formate is not shown after 210 min because of its broad line width and the noisy baseline.

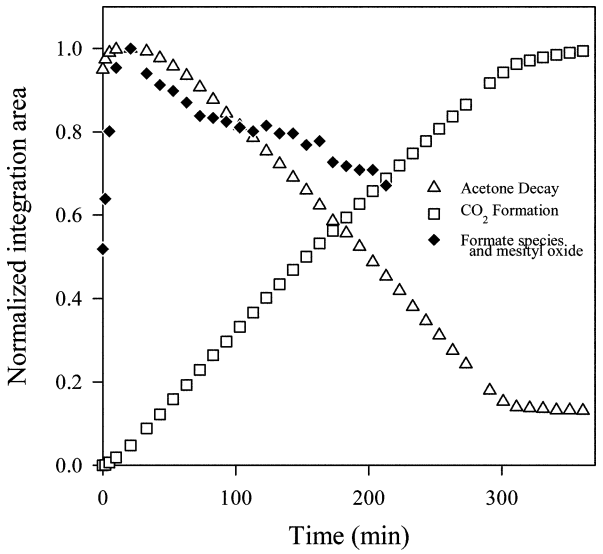

Figure 5. A representative kinetic curve for acetone PCO using the UV lamp as the irradiation source.

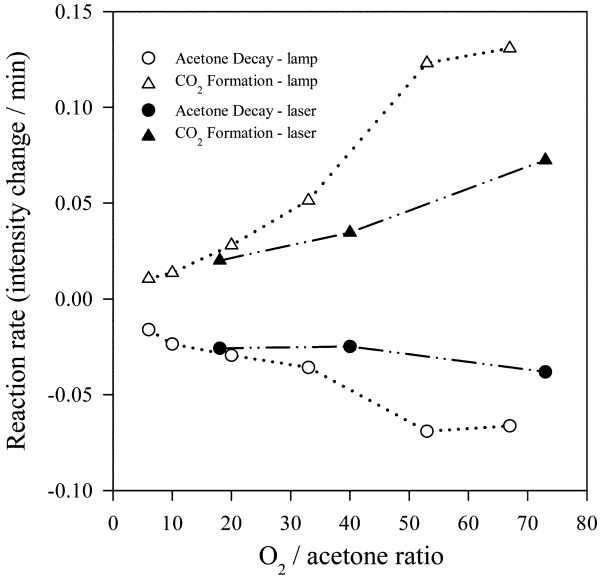

Figure 6. The reaction rate of different species as a function of oxygen concentration during acetone PCO. The data points with open symbols were obtained with the lamp source, while those with solid symbols were obtained with the laser source. Oxygen concentration is computed in terms of the oxygen/acetone ratio.

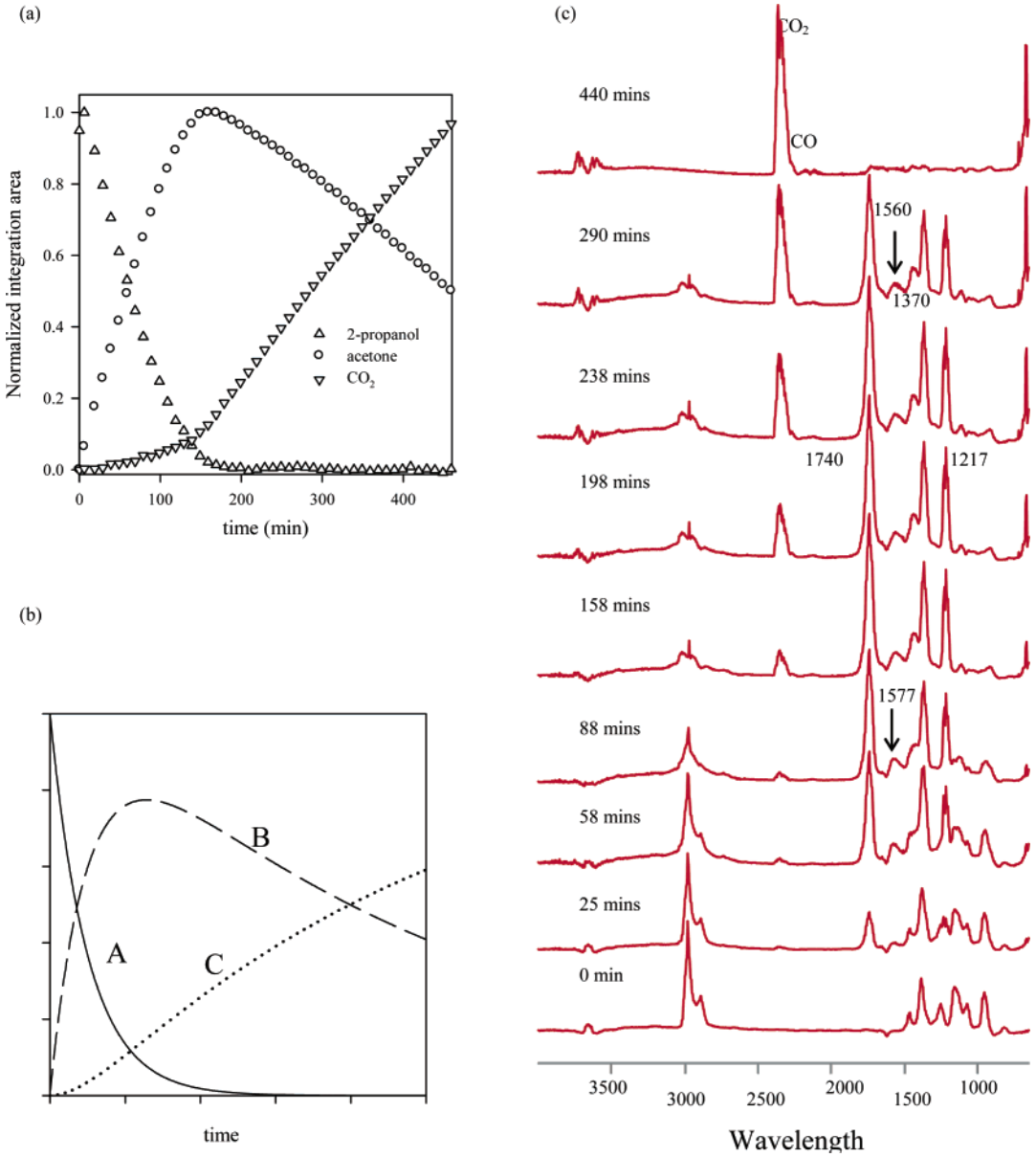

Figure 7. A representative kinetic curve (a) for 2-propanol PCO, (b) simulated kinetic curves for the consecutive reaction $A \xrightarrow{k_1} B \xrightarrow{k_2} C$ with $k_1/k_2 = 10$, and (c) typical spectra of 2-propanol PCO at different irradiation times (as specified) using the UV lamp source.

The observed formate species at the beginning of PCO is due to its formation from the thermal fragmentation of mesityl oxide. The formation of CO is not shown in the figure for clarity because the amount of CO formed was very small. As Figure 5 shows, the formation rate of CO_2 was almost constant before acetone was completely oxidized during acetone PCO. To compare the formation/decay rates of different species at various oxygen concentrations, the slopes for the linear portion of the kinetic traces in Figure 5 have been calculated. Note that the reaction rate is referred to as the change of integration intensity over the time in our calculation. These include the acetone decay rate and the CO_2 formation rate. The data points with the open symbols in Figure 6 show the reaction rate of acetone and CO_2 as a function of oxygen concentration with the continuous lamp UV source. As Figure 6 shows, the PCO rate of acetone increased nonlinearly as a function of oxygen concentration, the most obvious change occurring at an O_2/acetone ratio of 50. The extent of the rate change will be discussed in more detail herein in comparison to the PCO results using laser irradiation.

3.2.2.2. PCO of 2-Propanol. Spectra at different irradiation times for 2-propanol PCO using UV lamp irradiation are shown in Figure 7. The integration range for CO_2 is also 2400−2225 cm^{-1}. The integration range between 1880 and 1620 cm^{-1} includes a contribution from adsorbed acetone and mesityl oxide. The integration range for 2-propanol is 1000−880 cm^{-1} and therefore includes a contribution from 2-propoxide. The formation of CO is evident in the IR spectra at longer irradiation times but is not shown in the kinetic figure for clarity because of its low concentration. The kinetic plot in Figure 7a shows clearly that acetone is an intermediate in the 2-propanol PCO. However, the formation of CO_2 seems to proceed in two different stages: (1) before and (2) after the complete conversion of 2-propanol to acetone. A theoretical kinetic curve for the consecutive reaction of A to B and then to C is shown in Figure 7b and indicates the formation of final product C should be almost linear as a function of time during the whole process. Because the concentration of O_2 is much larger, the reaction within the system can be reasonably assumed to be pseudo-first-order in O_2 concentration. If the 2-propanol PCO simply proceeds

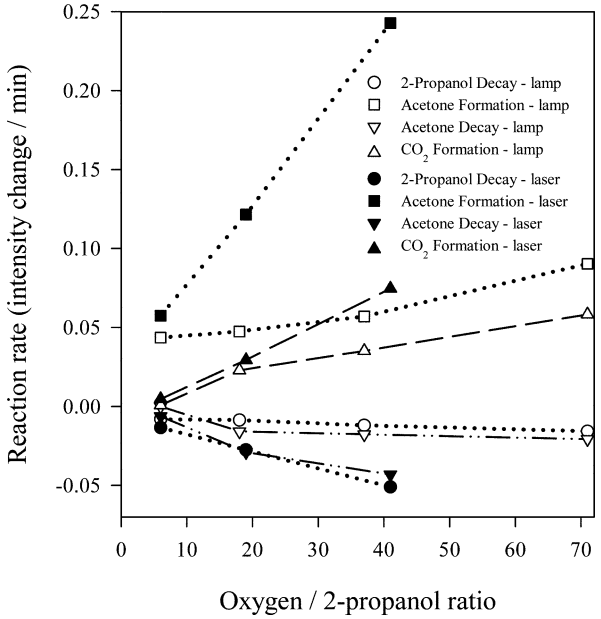

Figure 8. The reaction rate of different species as a function of oxygen concentration during 2-propanol PCO. The data points indicated by open symbols were obtained using the UV lamp, while those indicated by solid symbols were obtained with the laser source.

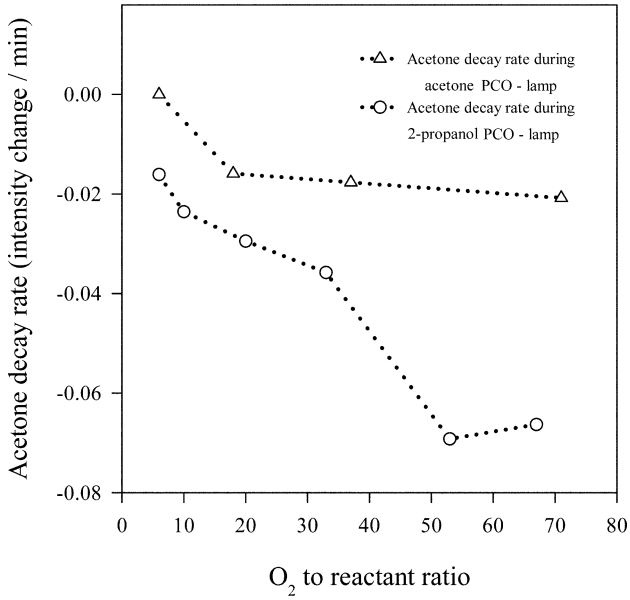

Figure 9. A comparison of the acetone decay rate during 2-propanol PCO and acetone PCO.

through acetone and then to final product CO_2, the CO_2 concentration should increase linearly or asymptotically with time during 2-propanol PCO, which is clearly contradictory to our observation. However, our SSNMR studies on 2-propanol PCO found that the 2-propoxide is much more active than H-bonded 2-propanol and can be directly oxidized to CO_2.[11] Therefore, the formation of CO_2 early in the PCO process is likely due to the direct oxidation of 2-propoxide. Another route through the further oxidation of acetone can contribute the formation of CO_2 during a second stage. The spectra in Figure 7 give some evidence for the presence of the intermediate mesityl oxide, as well as acetic acid (at 1450 cm^{-1}), which could form from its oxidation, as was observed previously.[12] The spectra in Figure 7 also show that the formate species at around 1560 cm^{-1} reaches a steady state (almost constant peak intensity), indicating that the formate species is an intermediate for the further oxidation of acetone to CO_2, as well during 2-propanol PCO. However, this route might not be very effective for rapid CO_2 formation (from 2-propoxide species) because the thermal equilibrium of formate species on TiO_2 powder is relatively slow. We have already seen that this equilibrium takes at least 30 min to achieve (see Figure 2).

To compare the formation/decay rates of different species at various oxygen concentrations, the slopes for the linear part in Figure 7 have also been calculated. The calculation is similar to that for acetone PCO. These reaction rates include the 2-propanol decay rate before its complete conversion, the acetone formation rate during 2-propanol conversion, the acetone decay rate after complete conversion of 2-propanol to acetone, and the CO_2 formation rate after the complete conversion of 2-propanol. The open symbols in Figure 8 show the reaction rate of 2-propanol, acetone, and CO_2 as a function of oxygen concentration with the continuous lamp UV source. As shown in the figure, the formation/decay rates of all species increased as the oxygen concentration increases. The extent of rate change will be discussed in more detail herein when we compare these results with those using laser irradiation.

It was also found that the decay rate of acetone as the intermediate of 2-propanol PCO was constantly slower than that during acetone PCO itself (see Figure 9). This difference in decay rate is much more obvious at high oxygen concentrations. This effect could result from a different distribution of species on the TiO_2 surface. In the case of acetone PCO, the surface was covered only by acetone and its derivatives. However, in the case of 2-propanol PCO, the surface species also include 2-propoxide and the produced H_2O, in addition to acetone and its degradation products. We expect that chemisorbed 2-propoxide has a larger affinity for surface adsorption sites than does H-bonded acetone. Although the O_2 concentration during acetone PCO was slightly higher than that during PCO of 2-propanol because of the consumption of O_2 in the conversion of 2-propanol to acetone, it is unlikely that this would cause the observed rate difference. This is because the O_2 concentration is much larger than either the acetone or the 2-propanol reactant concentrations and the consumption of O_2 should be small. A reaction scheme for the 2-propanol PCO is shown in Figure 10 and includes both the UV and thermal pathways for 2-propanol oxidation.

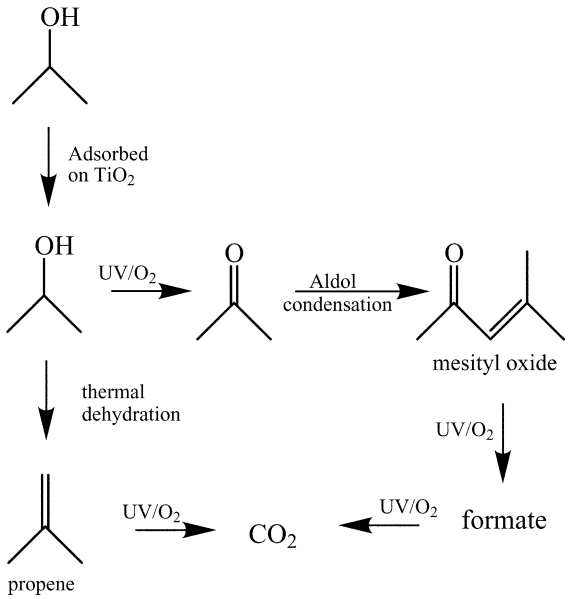

Figure 10. Illustration of the reaction mechanism for 2-propanol PCO on TiO_2 powder.

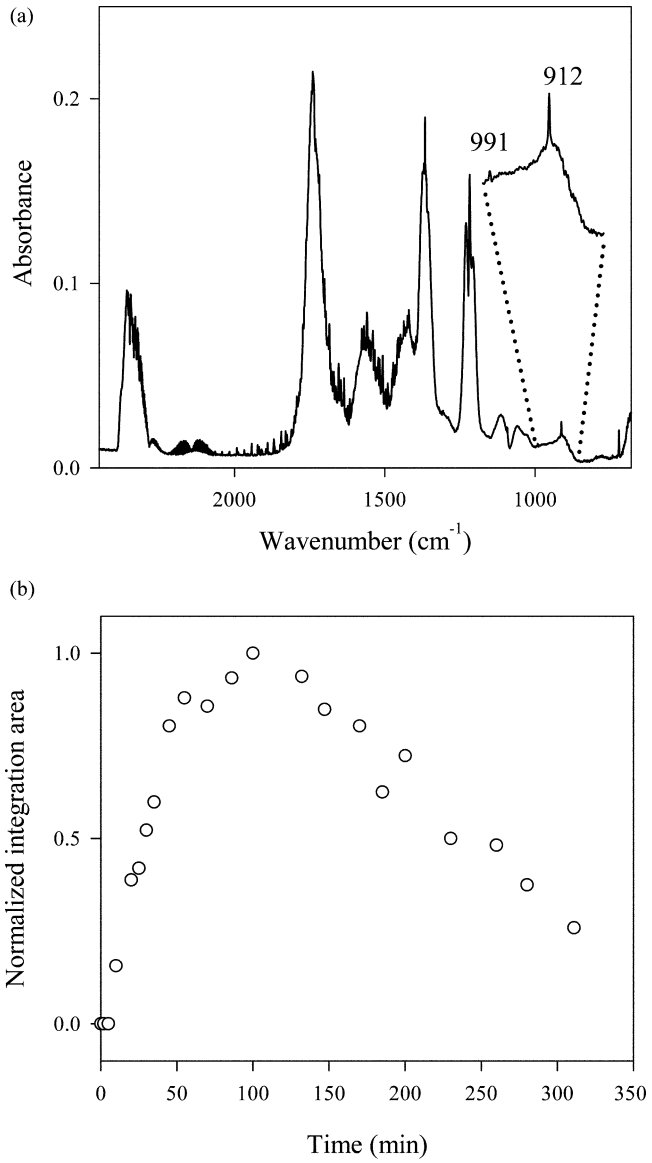

Figure 11. A typical spectrum (a) of 2-propanol PCO irradiated by a XeF laser showing the propene peak at 912 cm^{-1} and (b) a representative kinetic curve of propene during 2-propanol PCO using the laser as the irradiation source.

3.2.3. The UV Power Source. 3.2.3.1. Comparison of Laser and Lamp Source. In Figure 8, the formation/decay rates of different species during the 2-propanol PCO process using the XeF laser source are shown (solid symbols). The photon fluxes for the UV lamp and pulsed laser sources are comparable in these experiments as discussed above. In contrast to the lamp experiments, however, the reaction rate using the laser source was much greater for 2-propanol PCO. Furthermore, the reaction rate was almost linear with the concentration of oxygen concentration when using laser UV source. However, the effect of the laser source on the acetone PCO showed an opposite trend. As Figure 6 shows, the reaction rate with the laser source was always slower than that with lamp source at the same oxygen concentration.

Therefore, in comparison to UV lamp irradiation under similar photon fluxes, the laser source can increase the 2-propanol PCO rate while it reduces the acetone PCO rate. One possible explanation for this result is that the laser source may change the reaction mechanism. Our group reported the effect of the laser source on the PCO of CH_2Cl_2 and found that the pulsed laser irradiation changes the product state distribution and

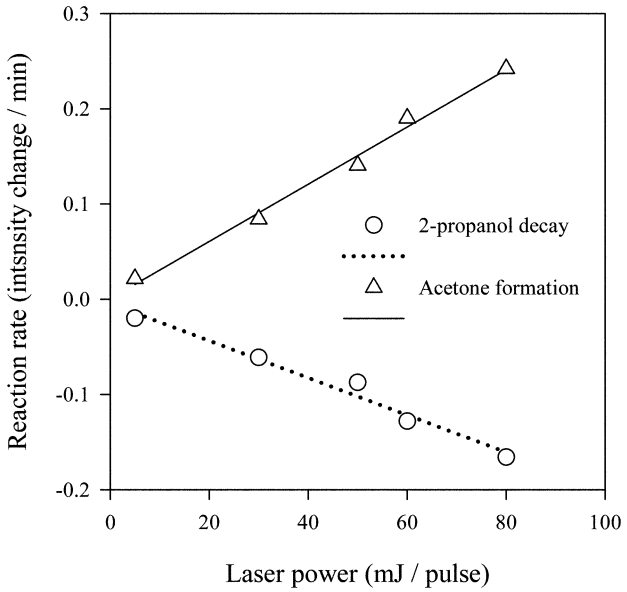

Figure 12. The 2-propanol degradation rate as a function of the laser power during 2-propanol PCO.

kinetics.[13] In this study, however, we did not observe many obvious changes in spectral characteristics during PCO of 2-propanol and acetone. However, we did observe characteristic peaks of propene at 991, 912, and 890 cm^{-1} as shown in Figure 11a, which consistently showed up in the case of 2-propanol PCO using laser irradiation. A kinetic plot is shown in Figure 11b. To explain the observed difference, we carried out a power study using the laser source to determine which of the following factors had an effect on 2-propanol PCO: multiphoton formation, a pulse effect, thermal heating, or a changed reaction mechanism.

3.2.3.2. Laser Power Study. 3.2.3.2.1. Multiphoton Effect. The multiphoton decomposition of gas-phase acetone has been investigated using a focused infrared laser at 9.68 μm.[27,28] To investigate whether multiphoton processes were important in our experiment, a series of different laser intensities was selected from 5 to 80 mJ/pulse using a repetition rate of 15 Hz. The rates of 2-propanol decay and formation of acetone as a function of laser pulse energy are shown in Figure 12. The figure shows that reaction rates of both 2-propanol decay and acetone formation during 2-propanol PCO are linear with the laser pulse intensity and indicates that multiphoton processes are not important in these experiments.

3.2.3.2.2. Pulse Effect. Previously, pulsed irradiation was applied to acetone photolysis to simplify its reaction by exclusively second-order radical reactions.[13,14] To explore whether the difference between results obtained with the laser and lamp sources in PCO studies of 2-propanol and acetone was due to the pulse effect, we simulated the pulse source by placing a chopper with same frequency as the laser (15 Hz) in front of the lamp. The result showed that the PCO rates of both 2-propanol and acetone were decreased simply because the powder density decreased. This indicates that the different effect of laser source on the PCO of 2-propanol and acetone was not simply due to the pulse effect.

3.2.3.2.3. Thermal Effect. A new product, propene, with the characteristic peaks at 991, 912, and 890 cm^{-1} was consistently observed during 2-propanol PCO at relatively high laser pulse energies (>50 mJ/pulse). The decomposition of 2-propanol can proceed along two paths by either dehydrogenation or dehydration, and its selectivity strongly depends on the reaction conditions, either thermally activated or photocatalytically

activated. In the PCO process, the dehydration process is favored.[8] Under thermal conditions, however, both acetone, a dehydrogenation product, and propene, a dehydration product, were found.[29,30] It has been estimated that the induced temperature change immediately following a laser pulse could be as high as a few thousand degrees using a tightly focused laser beam.[27,28] While we do not anticipate such high temperatures as those observed in ref 27 given our lower laser fluence, we do expect significantly elevated surface temperatures. We therefore ascribe the observed propene peaks under relatively high laser power as an indication that thermal reactions are present in the 2-propanol PCO process using pulsed laser irradiation. Through the kinetic plot of propene at 912 cm^{-1} during 2-propanol PCO as shown in Figure 11b, it clearly indicates that the propene is an intermediate as well. It is apparent that the laser source acts to change the reaction mechanism as compared to the continuous lamp source. In the case of 2-propanol, the abrupt temperature change induced by the laser source initiates its thermal dehydrogenation to the propene and the photocatalytic oxidation to acetone at the same time.

4. Conclusions

Photocatalytic reactions of 2-propanol and acetone on TiO_2 powder have been examined using two UV irradiation sources and in situ FTIR detection methods. The following conclusions can be derived from the above discussion: (1) The PCO of 2-propanol proceeds along two routes; one is through the chemisorbed species, 2-propoxide, and the other through the H-bonded 2-propanol. The route through 2-propoxide leads to a faster and direct oxidation to CO_2, while the route involving H-bonded 2-propanol proceeds through a conversion to acetone, formate species, and finally CO_2. (2) The PCO rates of 2-propanol and acetone are both increased as the oxygen concentration increases. The acetone decay rate during acetone PCO is much faster than that of acetone formed as an intermediate during 2-propanol PCO. (3) Both 2-propanol and acetone PCO show a dependence on the type of UV source used. The laser source increases the 2-propanol PCO rate, while it reduces the acetone PCO rate in comparison to the continuous lamp source. The abrupt temperature increase introduced by the high laser power irradiation makes a thermal decomposition route effective, which changes the reaction mechanism involving dehydrogenation of 2-propanol to form the propene intermediate. This is only involved with pulsed laser irradiation. No multiphoton processes were observed using the laser source.

Acknowledgment. The authors thank the NSF (Grant CHE-97-33188, CAREER grant) and the donors of Petroleum Research Fund, administered by the American Chemical Society, for funding this work. W. X. thanks Purdue's Environmental Science and Engineering Institute for a graduate fellowship.

References and Notes

(1) Fox, M. A.; Dulay, M. T. *Chem. Rev.* **1993**, *93*, 341.
(2) Hoffmann, M. R.; Martin, S. T.; Choi, W.; Bahnemann, D. W. *Chem. Rev.* **1995**, *95*, 69.
(3) Linsebigler, A. L.; Lu, G. Q.; Yates, J. T., Jr. *Chem. Rev.* **1995**, *95*, 735.
(4) Peral, J.; Ollis, D. *J. Catal.* **1992**, *136*, 554.
(5) Vorontsov, A. V.; Barannik, G. B.; Snegurenko, O. I.; Savinov, E. N.; Parmon, V. N. *Kinet. Catal.* **1997**, *38*, 84.
(6) Stevens, L.; Lanning, J. A.; Anderson, L. G.; Jacoby, W. A.; Chornet, N. *J. Air Waste Manage. Assoc.* **1998**, *48*, 979.
(7) Hager, S.; Bauer, R. *Chemosphere* **1999**, *38*, 1549.
(8) Larson, S. A.; Widegren, J. A.; Falconer, J. L. *J. Catal.* **1995**, *157*, 611.
(9) El-Maazawi, M.; Finken, A. N.; Nair, A. B.; Grassian, V. H. *J. Catal.* **2000**, *191*, 138.
(10) Raupp, G. B.; Junio, C. T. *Appl. Surf. Sci.* **1993**, *72*, 321.
(11) Xu, W.; Raftery, D. *J. Phys. Chem. B.* **2001**, *105*, 4343.
(12) Xu, W.; Raftery, D. *J. Catal.* **2001**, *204*, 110.
(13) Miller, M. L.; Borisch, J.; Raftery, D.; Francisco, J. S. *J. Am. Chem. Soc.* **1998**, *120*, 8265.
(14) Slagg, N.; Marcus, R. A. *J. Chem. Phys.* **1961**, *34*, 1013.
(15) March, R. E.; Polanyi, J. C. *Proc. R. Soc. London, Ser. A.* **1963**, *273*, 360.
(16) Basu, P.; Ballinger, T. H.; Yates, J. T., Jr. *Rev. Sci. Instrum.* **1988**, *59*, 1321.
(17) Wong, J. C. S.; Linsebigler, A.; Lu, G.; Fan, J.; Yates, J. T., Jr. *J. Phys. Chem.* **1995**, *99*, 335.
(18) Fan, J.; Yates, J. T., Jr. *J. Am. Chem. Soc.* **1996**, *118*, 4686.
(19) *Oriel Corporation Catalog*; 1994, Vol. II, pp 1−75.
(20) Panov, A.; Fripiat, J. J. *Langmuir* **1998**, *14*, 3788.
(21) Liao, L.-F.; Lien, C.-F.; Shieh, D.-L.; Chen, M.-T.; Lin, J.-L. *J. Phys. Chem. B* **2002**, *106*, 11240.
(22) Kubokawa, Y.; Miyata, H.; Wakamiya, M. *J. Phys. Chem.* **1973**, *77*, 141.
(23) Miyata, H.; Hata, K.; Nakajima, T.; Kubokawa, Y. *Bull. Chem. Soc. Jpn.* **1980**, *53*, 2401.
(24) *NIST WebBook*; National Institute of Standards and Technology: Gaithersburg, MD. http://webbook.nist.gov/.
(25) Nakajima, T.; Miyata, H.; Kubokawa, Y. *Bull. Chem. Soc. Jpn.* **1982**, *55*, 609.
(26) Popova, G. Ya.; Andrushkevich, T. V.; Chesalov, Yu. A.; Stoyanov, E. S. *Kinet. Catal.* **2000**, *41*, 805.
(27) Sato, H.; Nishio, S.; Kato, S.; Marumo, K.; Matsuzaki, A.; Yoshida, R. *Bull. Chem. Soc. Jpn.* **1996**, *69*, 3381.
(28) Brand, J. L.; George, S. M. *Surf. Sci.* **1986**, *167*, 341.
(29) Kim, K. S.; Barteau, M. A. *Langmuir* **1988**, *4*, 533.
(30) Rekoske, J. E.; Barteau, M. A. *J. Catal.* **1997**, *165*, 57.